

# Correction Method of The Cross-type Tensor Based on DA-LM

Caihong Li\*, Song Zhang

College of Electrical & Information Engineering, Southwest Minzu University, Chengdu 610041, China

**Abstract:** Magnetic sensor tensor system detection is a weak magnetic target detection. It requires high accuracy for the tensor system. In order to solve the problems of non-orthogonal error, scale factor error, zero error and non-alignment error in tensor system, a tensor error correction method based on DA-LM algorithm is proposed. Using tensor rotation invariance and the principle of scalar correction, a mathematical model including non-orthogonal error, scale factor error, zero error and non-alignment error is established, and the DA-LM algorithm is used to solve the unknown parameters of the equations. This method can not only estimate the parameters accurately. It can also calibrate the observed data to the orthogonal coordinates. The validity of the method is verified by simulation analysis and experiment. The error is reduced from 2500 nT to 0.15 nT in the simulation analysis and from 11000 nT to 200 nT in the experiment, and finally the position error is reduced from 13.15 m to 2.3217 m, which further verifies the validity of the correction algorithm.

**Keywords:** Magnetic sensor tensor system, Weak magnetic target, Scalar correction, DA-LM algorithm.

## 1. Introduction

As one of the earliest methods of geophysical exploration, due to its convenience, high efficiency, low cost and wide range of work, it has been widely used in geological exploration, underwater target location, space magnetic field detection, military anti-submarine, underground unexploded ordnance detection, medical endoscope location and so on [1-5]. At the same time, the technology of magnetic exploration has evolved from single sensor detection to sensor array detection, from magnetic field modulus detection to magnetic gradient detection and magnetic gradient tensor detection [6]. Compared to modulus and gradient detection, magnetic gradient tensor detection can provide deeper additional information of the magnetic field, which is not controlled by orientation error and is insensitive to spatial orientation and rotation noise. At the same time, it has a higher spatial resolution and is not easily affected by background magnetic interference and geomagnetic diurnal variation.

As early as the 1970s, foreign scientists had conducted research on magnetic gradient tensor detection. Since 1975, Wynn et al. proposed a magnetic target location method based on gradient tensor [7], the Institute of Physics and High Technology in Jena, Germany [8], the US Geological Survey [9], the Naval Surface Warfare Center [10-12], the Australian GSIRO agency [13], Singapore, Italy and other national research institutions have developed the fluxgate method triangular tensor system [14-15]. At the same time, the Chinese Academy of Sciences, such as the Shanghai Institute of Microsystems and Information, the Chinese Centre for Aeronautical Geophysics Survey and Remote Sensing under the Ministry of Land and Resources of the People's Republic of China, Chongqing University, China Shipbuilding Heavy Industry and Jilin University have also started to study the magnetic gradient tensor structure [16-26].

There are two common error correction methods for magnetic sensors: auxiliary vector correction and independent scalar correction. Auxiliary vector correction is performed by comparing the magnetic field vector with a

known one [29-30] and then making a reference correction to the magnetic sensor data, but in practice it is difficult to obtain a high accuracy magnetic field vector. Independent scalar correction, does not require a known magnetic field vector, it uses a constant value of the magnetic field as a constraint for its correction. Independent scalar method is most commonly used in magnetic sensor array error correction for the two-step correction method [31], which means that the first correction of a single sensor non-orthogonal, scale factor, zero bias error, then the non-alignment error is corrected, and the magnetic field modulus is constant in both steps. A correction method based on the invariance of the magnetic gradient tensor has also been proposed by [32], but the correction algorithm used in this paper is sensitive to the initial values, making it easy to fall into local minima when solving for the parameters. On this basis, this paper proposes a method for error correction of magnetic sensor arrays based on the DA-LM algorithm.

The structure of this paper is as follows: Chapter 1 introduces the development stage of magnetic exploration technology, the magnetic tensor detector and the general development status of error correction; Chapter 2 first analyses the error sources of the magnetic sensor array, establishes the error calibration model, and then introduces the basic principle and implementation steps of the DA-LM algorithm; Chapter 3 demonstrates the effectiveness of the algorithm in the tensor correction process through simulation experiments and real measurement experiments, respectively; Chapter 4 summarises the work done in this paper.

## 2. Methodology

### 2.1. Sensor array error model analysis

Magnetic detection technology has evolved from modal detection and gradient detection to magnetic gradient tensor detection, which has attracted the attention of researchers because it is not limited by total field measurement, can effectively respond to the vector information of magnetic targets, is not controlled by orientation errors, is insensitive to spatial orientation and rotation noise, has higher spatial resolution, and is not easily affected by background magnetic

interference from the environment and daily geomagnetic variations. The most common tensor structures are triangular, cross, square, orthotetrahedral and right-angled tetrahedral. In practice, the magnetic gradient tensor is obtained using the difference approximation rather than the partial differential approximation, but the tensor system has different tensor formulae for different structures. In the literature [33], Liu Limin et al. listed the tensor formulae for several common structures and analysed the errors of the five independent components of the tensor under different structures, and concluded that the one with the smallest error was the cross-type tensor structure.

The magnetic sensor tensor system is the basis for the application of weak magnetic target localisation and the accuracy of the localisation is directly dependent on the accuracy of the magnetic sensor tensor system measurements. The magnetic gradient tensor for practical applications is obtained using the differential approximation rather than the partial differential approximation and therefore requires even higher accuracy from the tensor system. Individual magnetic sensors have non-orthogonality, scale factor and zero bias errors, and when multiple sensors are short-circuited together there is a mounting error between the magnetic sensors, which combined with the effects of the external environment can make tensor measurement errors of thousands of nanometres, so the sensor array must be carefully calibrated before use.

In the presence of both the magnetic sensor inherent error and the misalignment error, the relationship between the magnetic field test value and the ideal value can be expressed as:

$$B_m = TLAB_i + B_0 \quad (1)$$

where  $A$  denotes non-orthogonal error,  $L$  denotes the scale factor error,  $T$  denotes non-alignment error,  $B_0$  denotes zero bias error. The  $(TLA)^{-1}$  is then replaced by  $P$  and  $-(TLA)^{-1}B_0$  by  $Q$ . The deformed form is then:

$$B_i = PB_m + Q \quad (2)$$

The magnetic gradient tensor is the rate of change of the three components of the magnetic sensor,  $B_x$ ,  $B_y$  and  $B_z$ , in the  $x$ ,  $y$  and  $z$  axes, denoted as  $B_{xx}$ ,  $B_{xy}$ ,  $B_{xz}$ ,  $B_{yx}$ ,  $B_{yy}$ ,  $B_{yz}$ ,  $B_{zx}$ ,  $B_{zy}$  and  $B_{zz}$ , and is called the second order tensor  $G$  of the magnetic scalar potential.

$$G = \begin{bmatrix} \frac{\partial B_x}{\partial x} & \frac{\partial B_x}{\partial y} & \frac{\partial B_x}{\partial z} \\ \frac{\partial B_y}{\partial x} & \frac{\partial B_y}{\partial y} & \frac{\partial B_y}{\partial z} \\ \frac{\partial B_z}{\partial x} & \frac{\partial B_z}{\partial y} & \frac{\partial B_z}{\partial z} \end{bmatrix} = \begin{bmatrix} B_{xx} & B_{yx} & B_{zx} \\ B_{xy} & B_{yy} & B_{zy} \\ B_{xz} & B_{yz} & B_{zz} \end{bmatrix} \quad (3)$$

For a quasi-static field in a non-conducting medium, the magnetic field has a dispersion and a spin of 0, i.e.  $\nabla \times B = 0$ ,

$\nabla \cdot B = 0$ . This means that 5 of the 9 elements of the magnetic gradient tensor are independent, and then  $G$  can be rewritten as:

$$G = \begin{bmatrix} B_{xx} & B_{xy} & B_{xz} \\ B_{xy} & B_{yy} & B_{yz} \\ B_{xz} & B_{yz} & -B_{xx} - B_{yy} \end{bmatrix} \quad (4)$$

Furthermore, a very important feature of the magnetic gradient tensor are the derived tensor invariants, which do not change with rotation of the coordinate axes. In a uniform magnetic field all tensor invariants are zero, in a non-uniform field they are all non-zero constants except  $I_0$ .

$$\begin{aligned} I_0 &= B_{xx} + B_{yy} + B_{zz} = 0 \\ I_1 &= B_{xx}B_{yy} + B_{yy}B_{zz} + B_{zz}B_{xx} - B_{xy}^2 - B_{yz}^2 - B_{xz}^2 \\ I_2 &= \det(G) = B_{xx}B_{yy}B_{zz} - B_{xx}B_{yz}^2 - B_{zz}B_{xy}^2 - B_{yy}B_{xz}^2 + 2B_{xy}B_{xz}B_{yz} \\ C_T &= \sqrt{\sum_{i,j=x,y,z} B_{ij}^2} = \sqrt{-2I_1} \end{aligned} \quad (5)$$

The schematic diagram of the magnetic gradient tensor structure is shown in Figure 1. The system coordinates are set as follows: the centre of the array is the origin, the  $x$ -axis is along the direction from magnetic sensor 3 to 1, the  $y$ -axis is along the direction from magnetic sensor 4 to 2 and the  $z$ -axis is up. The gradient field is approximated by the difference in values between two separated magnetometers. In this case, the modified gradient field can be expressed in vector form as:

$$\begin{aligned} G_x &= \frac{1}{L} [B_1 - (P_3B_3 + Q_3)] \\ G_y &= \frac{1}{L} [B_2 - (P_4B_4 + Q_4)] \end{aligned} \quad (6)$$

where  $G_x$  is the vector  $\begin{pmatrix} B_{xx} \\ B_{yx} \\ B_{zx} \end{pmatrix}$  and  $G_y$  is the vector  $\begin{pmatrix} B_{xy} \\ B_{yy} \\ B_{zy} \end{pmatrix}$ . The cross-shaped structure has no sensor in the  $z$ -

direction, so the gradient field along the  $z$ -axis is calculated from the symmetry of the magnetic gradient tensor.

So the expression of the tensor invariant  $I_1$  is:

$$I_1 = f(B_{xx}, B_{yx}, B_{zx}, B_{xy}, B_{yy}, B_{zy}) = f(P_3^{3 \times 3}, Q_3^{3 \times 1}, P_4^{3 \times 3}, Q_4^{3 \times 1}) \quad (7)$$

The basic principle of this correction method is that the tensor system rotates with its centre and the tensor invariants are all a constant. All parameters are estimated by minimising the residuals at  $N$  sampling points during the rotation, with the objective function set to:

$$y = \min \sum_{i=1}^N \left| f_i \left( P_3^{3 \times 3}, Q_3^{3 \times 1}, P_4^{3 \times 3}, Q_4^{3 \times 1} \right) - c \right|^2 \quad (8)$$

Equation (8) is a non-linear function with 24 correction parameters and one constant. The 24 correction parameters are solved by the DA-LM algorithm.

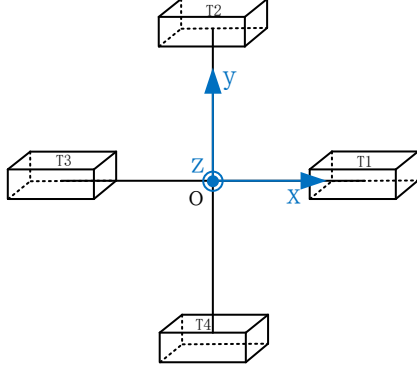


Figure 1. Structure of the cross tensor structure

## 2.2. Principle of the DA-LM error correction algorithm

### (1) LM algorithm

The LM algorithm is a modification of Newton's algorithm. It solves the problem that Newton's algorithm cannot guarantee that the search direction is always descending and the Hessian matrix is always positive definite. The basic idea of Newton's method is to use the first and second order derivatives at iteration  $x_k$  to make a quadratic approximation to the objective function, then use the quadratic model minima as new iteration points and repeat the process until an approximate minimum that satisfies the accuracy is found. When the objective function:  $f: R^n \rightarrow R$  is second-order continuously differentiable, during the Taylor expansion of the function  $f$  at point  $x_k$ , the terms are ignored more than three times, and the quadratic approximation function can be obtained as follows:

$$f(x) \approx f(x_k) + (x - x_k)g(x_k) + \frac{1}{2}H(x_k)(x - x_k)^2 \quad (9)$$

where  $g(x_k) = \nabla f(x_k)$  denotes the first-order derivative of  $f$  at point  $x_k$ ,  $H(x_k) = \nabla^2 f(x_k)$  denotes the second-order derivative of  $f$  at point  $x_k$ . If we apply the necessary condition for local minima of the first order to this, we obtain:

$$\nabla f(x) = g(x_k) + H(x_k)(x - x_k) = 0 \quad (10)$$

If  $H(x_k) > 0$ , the minimum point of the function  $f$  is:

$$x_{k+1} = x_k - H(x_k)^{-1}g(x_k) \quad (11)$$

This is the iterative formula of Newton's method. In the case of a single variable, Newton's method does not converge to a minimum point if the second derivative of the function

$f'' < 0$ . In the multivariate case, if the Hessian matrix  $H(x_k)$  of the objective function is non-positive, the search direction determined by Newton's method is not necessarily the direction in which the value of the objective function decreases. To solve the above problem, introduce the damping factor  $\mu \geq 0$  and modify the iterative equation as:

$$x_{k+1} = x_k - (H(x_k) + \mu_k I)^{-1}g(x_k) \quad (12)$$

As long as  $\mu$  is large enough, it is always guaranteed that the search direction  $d_k = -(H(x_k) + \mu_k I)^{-1}g(x_k)$  is a descent direction. This is the iteration formula of the LM algorithm.

### (2) DA algorithm

The DA algorithm is a bionics algorithm proposed in 2016 by Mirjalili. The main idea comes from the static foraging behavior and dynamic migration behavior of dragonflies in nature. In static swarms, small groups of dragonflies fly back and forth over a small area in search of other flying prey, and local movements and temporary changes in flight path are characteristic of static swarms. In dynamic groups, large groups of dragonflies migrate long distances in a common direction and against the prevailing wind to find better living conditions. The algorithm uses the dragonflies' habits to classify them into five categories of behaviour: separating, lining up, aligning, finding prey and avoiding natural predators. The separation weight, orientation weight, coalescence weight, prey weight factor and natural enemy weight factor in the algorithm are used as the dragonfly's behavioural degrees to update the dragonfly's position, and the algorithm is able to improve the initial random parameters of a given problem to converge to a global optimum.

Mathematical expression for the DA algorithm:

$$\Delta X_{t+1} = (s \times S_i + a \times A_i + c \times C_i + f \times F_i + e \times E_i) + \omega' \times \Delta X_t \quad (13)$$

where  $s$  is the separation weight,  $a$  is the alignment weight,  $c$  is the cohesion weight,  $f$  is the prey weight factor,  $e$  is the natural enemy weight factor,  $t$  is the number of current iterations, and  $\omega'$  is the inertia weight;  $S_i$  is the position vector for the separation behaviour of the  $i$ th dragonfly,  $A_i$  is the position vector for the queuing behaviour of the  $i$ th dragonfly,  $C_i$  is the position vector for the alliance behaviour of the  $i$ th dragonfly,  $F_i$  is the position vector for the hunting behaviour of the  $i$ th dragonfly and  $E_i$  is the position vector for the avoidance behaviour of the  $i$ th dragonfly.

In nature, dragonflies are on the move most of the time for survival reasons. Therefore, their position has to be updated in real time. So there are:

$$X_{t+1} = X_t + \Delta X_{t+1} \quad (14)$$

Although the LM algorithm can solve for multiple unknowns simultaneously, there is still a risk of falling into local minima if the initial values are not chosen appropriately, which can affect the accuracy of the solution. The DA

algorithm, as a global search algorithm, uses its strong global search capability to find the global best position, and then uses its output parameter values as initial values for the LM

algorithm, which performs the local search. Figure 2 shows the specific flow of the DA-LM algorithm.

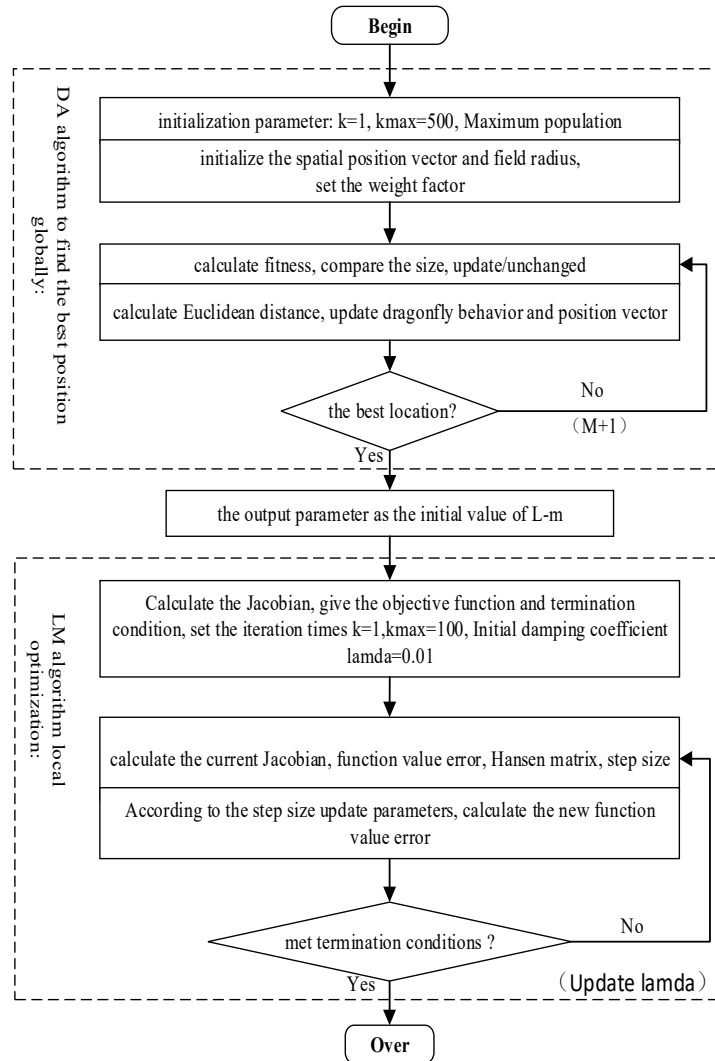


Figure 2. The flows of the DA-LM algorithm

### 3. Results and Discussion

#### 3.1. Simulation analysis

Now suppose there is a uniform field with a background magnetic modulus  $B = 55000$  nT, a magnetic inclination  $I = -5^\circ$  and a magnetic declination  $D = 60^\circ$ . The simulation experiment diagram is shown in Figure 1, let its x-axis positive direction pointing due east (E), y-axis positive direction pointing due north (N), z-axis up, baseline  $L = 0.2$ m,

sensors 1 and 3 are parallel to the x-axis and pointing from sensor 3 to sensor 1, sensors 2 and 4 are parallel to the y-axis and pointing from sensor 4 to sensor 2. It is assumed that the coordinate system of the four sensors is the same as the coordinate system of the cross-shaped magnetic sensor array structure. According to the uniform field, the magnetic field measured by each sensor is the same size, and then rotated around the x-axis, y-axis and z-axis respectively to obtain 360 sets of data after rotation, the rotation operation is shown in Figure 3.

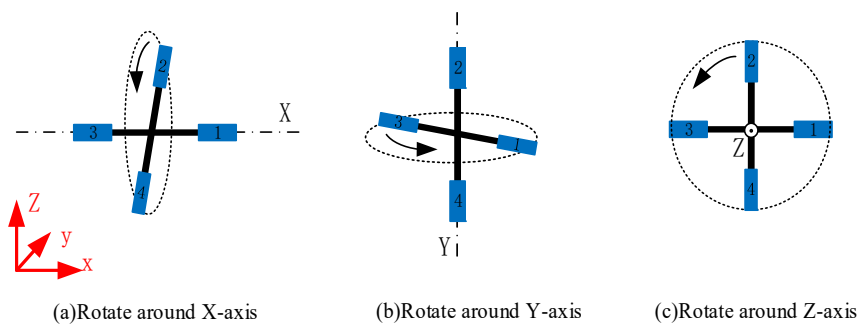
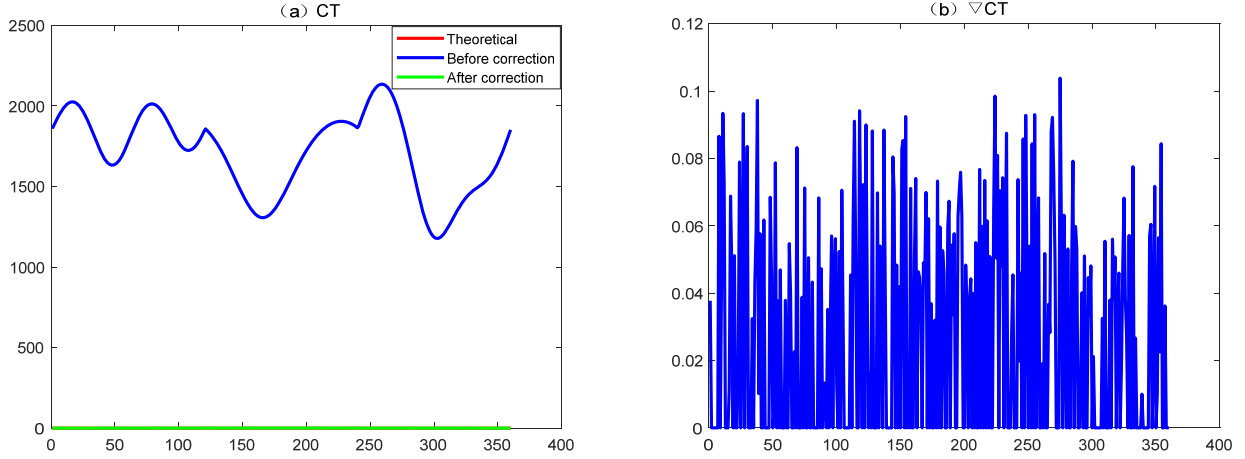


Figure 3. Schematic diagram of rotary operation

After rotating to obtain 360 data sets, the G matrix of the sensor centroids, as well as  $I_l$  and  $C_T$ , are solved using differential approximation. As shown in equation (5), there is a quadratic relationship between  $I_l$  and  $C_T$ , so only one needs to be chosen to analyse calibration performance, with the ideal  $C_T=0$  in a uniform field. Now set the non-

orthogonal, scale factor, zero bias and non-alignment parameters of each error, generate the corresponding test data, calculate the  $C_T$  value with error, and then use the DA-LM algorithm proposed in this paper for error correction, the  $C_T$  value before and after correction is shown in Figure 4, the preset parameter values and DA-LM predicted values are shown in Table 1.



**Figure 4.** Schematic diagram of rotary operation

It can be seen in Figure 4 that the  $C_T$  measured by the sensor array with errors in the uniform field ranges from 1000nT to 2500nT, with an ideal value of 0, while the magnetic gradient tensor invariant  $C_T$  drops to 0nT after

correction by the DA-LM algorithm. The difference between the corrected  $C_T$  value and the ideal value is only 0 to 0.15 nT, indicating that the DA-LM algorithm is effective in correcting for tensor-invariant  $C_T$ .

**Table 1.** Parameter defaults and DA-LM estimates

Parameter	Preset values	DA-LM estimates
$P_3$	$\begin{bmatrix} 1.005299 & -0.001392 & 0.001493 \\ 0.001563 & 1.005903 & 0.000238 \\ -0.001224 & 0.000889 & 1.004697 \end{bmatrix}$	$\begin{bmatrix} 1.002217 & -0.001124 & 0.001309 \\ 0.001016 & 1.000229 & -0.000055 \\ -0.001219 & 0.000955 & 0.998851 \end{bmatrix}$
$Q_3$	$\begin{bmatrix} 74.904786 \\ -21.269311 \\ -11.136718 \end{bmatrix}$	$\begin{bmatrix} 100.000002 \\ -52.679788 \\ -11.028415 \end{bmatrix}$
$P_4$	$\begin{bmatrix} 0.998299 & -0.001096 & 0.001940 \\ 0.000447 & 1.001201 & -0.000635 \\ -0.001309 & 0.000391 & 0.998899 \end{bmatrix}$	$\begin{bmatrix} 0.998755 & -0.000956 & 0.001258 \\ 0.000208 & 1.000724 & -0.000564 \\ -0.000842 & 0.000298 & 0.998738 \end{bmatrix}$
$Q_4$	$\begin{bmatrix} -28.992672 \\ 113.791501 \\ 79.066059 \end{bmatrix}$	$\begin{bmatrix} 16.908453 \\ 99.232721 \\ 100.000002 \end{bmatrix}$

The above simulation analysis shows that the DA-LM correction algorithm proposed in this paper is applicable to both non-uniform and uniform fields. The effectiveness of the algorithm proposed in this paper will be further verified by practical experiments later on.

### 3.2. Experimentation

Magnetic sensors are extremely sensitive to changes in the surrounding magnetic field and therefore need to find an open, flat area in the field with little variation in the magnetic field. In addition to the magnetic sensor itself and installation errors,

the solar magnetic variation also has a large influence on the measurement of the magnetic sensor, and the experimental time was chosen at night when the solar magnetic variation has less influence. The non-magnetic turntable is placed on a flat surface and a 20cm cross-shaped non-magnetic aluminium frame is mounted on the non-magnetic turntable. The non-magnetic aluminium cross frame is marked 1, 2, 3 and 4. A coordinate system for the magnetic sensor array is established as shown in Figure 1 and the initial state is aligned with the geographic coordinates. The positive y-axis is oriented to geographic north, the positive x-axis is oriented to

geographic east and the positive z-axis is oriented vertically upwards. As there are only two three-axis magnetic sensors, the measurement of this cross-shaped sensor array is performed in two steps, with the two sensors placed in positions 1 and 3, and then in positions 2 and 4 of the cross-shaped non-magnetic aluminium frame. The coordinates of the three-axis magnetic sensors are aligned with the array coordinate system, while the magnetic field modal values are recorded using a high precision proton magnetometer to continuously monitor the magnetic field changes in the field. The overall field calibration setup is shown in Figure 5.



**Figure 5.** Diagram of the experimental set-up for the field calibration

After the calibration experimental platform was built, the vertical axis of the turntable was first fixed and the horizontal axis was rotated for one week to collect data, then the angle of the vertical axis was changed and the horizontal axis was rotated for another week to collect data. 46 sets of three-component magnetic field data were collected in this rotational manner. The tensor components were calculated according to the tensor formula of the cross-shaped tensor structure, and then the  $C_T$  values of the actual test data were calculated, and the  $C_T$  values before and after correction are shown in Figure 6.

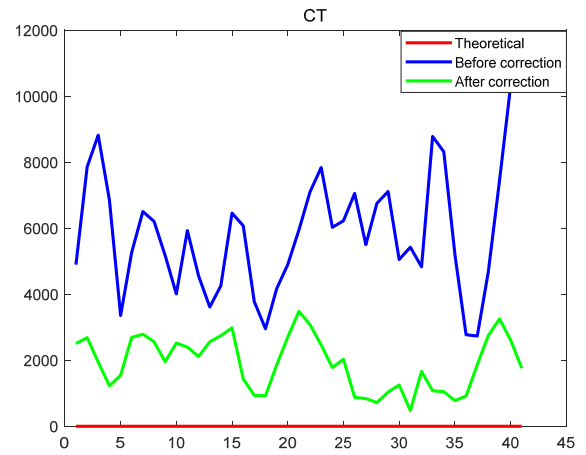


**Figure 6.**  $C_T$  values before and after correction

As can be seen in Figure 6, the DA-LM algorithm reduces the CT values in the real measurement from 11000nT to 2000nT, indicating that the correction algorithm proposed in this paper is effective. However, the experimental environment is not a uniform and constant magnetic field, and there will be factors such as interference from magnetic sources, and the error model established in this paper does not fully cover all errors.

### 3.3. Positioning experiment

To further demonstrate that the DA-LM algorithm is effective for error correction of the cross-shaped tensor structure, a comparison of the positioning effect before and after correction is next made using the TMG improved positioning method proposed by Xiaoyu Tang [31]. The detection target uses a rectangular permanent magnet with a modulus value of  $2A/m^2$  and the positioning platform and calibration are consistent. The positioning results before and after calibration are shown in Table 2.

**Table 2.** Positioning effect before and after correction

Real position		TMG calculated value	Three component error	Distance error/m
Before correction	1.25	-4.7869	-6.0369	13.1500
	1.285	7.5782	6.2932	
	-0.75	9.0942	9.8424	
After correction	1.25	-0.4945	-1.7445	2.3217
	1.285	2.2478	0.9628	
	-0.75	-1.9415	-1.1915	

The positioning data in Table 2 shows that the correction method proposed in this paper reduces the positioning error from 13.15m to 2.3217m, which indicates that the correction method proposed in this paper is helpful in improving the positioning accuracy and proves the effectiveness of the method in this paper.

## 4. Conclusion

This paper presents an integrated correction method based on the relationship that the invariants of the magnetic gradient tensor do not vary with the coordinate system. An error correction model is first developed, then a parameter solution algorithm is proposed, and finally the error parameters are used to directly correct the output values of the magnetic gradient tensor system. Simulation results show that the

improvement rate of the method is as high as 95%, and practical experiments verify the feasibility of the method, but there is a certain decrease in the improvement rate due to the influence of the measurement environment, etc. The method proposed in this paper is also applicable to other structural types of magnetic gradient tensor systems and provides the basis for further applications of magnetic anomaly data at a later stage.

## Acknowledgment

This project was supported by the Innovative Research Project for Graduate Students of Southwest Minzu University (Project No.YB2022703).

## References

- [1] Yanliang Yuan, Baohua Liu and Guien Zhang(2005). Application of Magnetic Method to Ocean Engineering. *Advances in Marine Science*, no.01, p.114-119.
- [2] Jian Zhang, Chunsheng Lin and Fan Huang(2011). Application of OBF Decomposition and BP Neural Network to Magnetic Signal Detection of a Ship. *Marine Electric & Electronic Engineering*, vol.31, no.07, p.13-16.
- [3] Jinyong Ma(2018). Application of high precision magnetic prospecting in regional investigation. *World Nonferrous Metals*, no.07, p.148-149.
- [4] Sheng Cai(2018). The Application of Geophysical Magnetic Exploration in Railway Surveying. *Railway Investigation and Surveying*, vol.44, no.01, p.88-91.
- [5] Han Song, Liang Zou and Xiuqun Zhang(2019). Inter-Turn Short-Circuit Detection of Dry-Type Air-Core Reactor Based on Spatial Magnetic Field Distribution. *Transactions of China Electrotechnical Society*, vol.34, no.s1, p.105-117.
- [6] Changda Zhang(2007). Some Problems Concerning the Magnetic Anomaly Detection. *Chinese Journal of Engineering Geophysics*, vol.06, no.06, p.549-553.
- [7] W. Wynn, C. Frahm and P. Carroll(1975). Advanced superconducting gradiometer/Magnetometer arrays and a novel signal processing technique. *IEEE Transactions on Magnetics*, vol.11, no.02, pp.701-707.
- [8] R. Stolz, V. Zakosarenko and M. Schulz(2006). Magnetic full-tensor SQUID gradiometer system for geophysical applications. *The Leading Edge*, vol.25, no.02, p.178-180.
- [9] Robert E B, Smith D V and Brown P J(2005). Calibrating a tensor magnetic gradiometer using spin data. *Reston VA US*.
- [10] R. Wiegert, B. Price and J. Hyder(2002). Magnetic anomaly sensing system for mine countermeasures using high mobility autonomous sensing platforms. *OCEANS '02 MTS/IEEE*, vol.02, p.937-944.
- [11] Roy F and Wiegert. Man-Portable Magnetic Scalar Triangulation and Ranging System for Detection. *Localization and Discrimination of UXO*.
- [12] Allen G I, Sulzberger G and Bono J T(2005). Initial evaluation of the new real-time tracking gradiometer designed for small unmanned underwater vehicles. *IEEE*.
- [13] Keenan S T, Young J A and Foley C P(2010). A high- T c flip-chip SQUID gradiometer for mobile underwater magnetic sensing. *Superconductor Science Technology*, vol.23, no.02, p.24.
- [14] Pei Y H, Yeo H G and Kang X Y(2010). Magnetic gradiometer on an AUV for buried object detection. *IEEE*, p.1-8.
- [15] Cocchi L, Carmisciano C and Palangio P(2015). S3MAG - Low magnetic noise AUV for multipurpose investigations. *IEEE*.
- [16] Ying Wang, Longqing Qiu and Wen Shi(2015). Study on Compensation of Unbalance of Full-Tensor LTS-SQUID Magnetic Gradiometer. *Low Temperature Physical Letters*, vol.37, no.03, p.169-173.
- [17] Zhao J, Wang J and Liu G(2009). Axial high-temperature rf SQUID gradiometer system for geomagnetic prospecting. *Electronic Measurement & Instruments*, no.01, 704-707.
- [18] Jing Zhao, Guangda Liu and Zhanfeng An(2011). Design and Implementation of Measurement and Control System for HTS SQUID Gradiometer. *Computer Measurement & Control*, vol.19, no.05, p.1052-1054.
- [19] Yin Gang, Zhang Yingtang and Fan Hongbo(2015). Linear calibration method of magnetic gradient tensor system. *Measurement*, vol.45, no.03, p.1012-1016.
- [20] Yu Zhao, Jin Zhang and Ruihui Deng(2014). The RS-HC3 System of Marine Tensor Magnetic Gradient and Its Application. *Hydrographic Surveying and Charting*, vol.34, no.02, p.25-27.
- [21] Yangyi Sui, Guang Li and Wang Shilong(2014). Compact fluxgate magnetic full-tensor gradiometer with spherical feedback coil. *The Review of scientific instruments*, vol.85, no.01, p.75-77.
- [22] Yangyi Sui, Hongsong Miao and Yanzhang Wang(2016). Correction of a Towed Airborne Fluxgate Magnetic Tensor Gradiometer. *Remote Sensing Lett*, vol.13, no.12.
- [23] Sheng D, Perry A R and Krzyzewski S P(2017). A microfabricated optically-pumped magnetic gradiometer. *Applied Physics Letters*, vol.110, no.03, p.1106-1109.
- [24] Jin H H, Zhuang Z H and Wang H B(2018). None-Asphericity-Error Method for Magnetic Dipole Target Detection. *IEEE Geoscience and Remote Sensing Letters*, vol.15, no.08, p.1-5.
- [25] Jin H, Guo J and Wang H(2020). Magnetic Anomaly Detection and Localization Using Orthogonal Basis of Magnetic Tensor Contraction. *IEEE Transactions on Geoscience and Remote Sensing*, vol.58, no.8, pp.5944-5954.
- [26] Xiaoqian Duan, Dongxing Pei and Peng Yuan(2019). Single Point Positioning Method Based on Magnetic Moment Gradient Tensor. *Journal of Ordnance Equipment Engineering*, vol.40, no.08, p.165-169.
- [27] Qingzu Li, Zhining Li and Yingtang Zhang(2017). Two-step linear calibration of planar cross magnetic gradient tensor system. *Chinese Journal of Scientific Instrument*, vol.38, no.09, p.2232-2242.
- [28] Gebre Egziabher, Demoz Elkaïm and G Powell(2022). A non-linear, two-step estimation algorithm for calibrating solid-state strapdown magnetometers.
- [29] Xiang Li and Zhi Li(2012). Dot product invariance method for the calibration of three-axis magnetometer in attitude and heading reference system. *Chinese Journal of Scientific Instrument*, vol.33, no.08, p.1813-1818.
- [30] Xiang, Li, Baiqi(2018). Researchers from Guilin University of Electronic Technology Discuss Findings in Sensor Research (Calibration and Alignment of Tri-Axial Magnetometers for Attitude Determination). *Journal of Technology & Science*.
- [31] Xiaoyu Tang, Li Yang and Chaoqun Xu(2021). Study on Calibration Method of Three-Axis Magnetic Sensor Based on Gaussian Process Regression. *Chinese Journal of Sensors and Actuators*, vol.34, no.10, p.1340-1345.
- [32] Mu Y, Wang C and Zhang X(2018). A Novel Calibration Method for Magnetometer Array in Nonuniform Background

- Field. IEEE Transactions on Instrumentation and Measurement, no.99, p.1-9.
- [33] Limin Liu(2012). Configuration Design , Error Analysis and Underwater Target Detection of Fluxgate Tensor Magnetometer. JILIN University, p.10-23.
- [34] Weimin Wu, Wangyang Wu and Zhiyi Lin(2017). Dragonfly algorithm based on enhancing exchange of individuals' information. Computer Engineering and Applications, vol.53, no.02, p.223-231.
- [35] Meiyong Qiao, Chengkuan Xu and Xiaxia Tang(2021). Application research of DA-LM Algorithm in Error Correction of MEMS Accelerometer. Chinese Journal of Sensors and Actuators, vol.34, no,02, p.223-231.